STIMULATED RESULTS

Pseudo-Code:

The following is code for the stimulation that is implemented in Matlab.

```
BEGIN

    DEFINE constants: J_m = 6.7e-4 m2 = 0.190276, m3 = 0.198764, m4 = 0.306845
r2 = 0.0682, r4 = 0.1451 J2 = 407.655e-6, J3 = 3503.14e-6, J4 = 3673.87e-6 a2 = 0.09, a3
= 0.36, a4 = 0.26 p = 0.18, q = 0.0 Kt = 0.76 Ke = 90 * (1/60) L = 5.8e-3 R = 0.8 n_max =
3000 Ts = 10.2 Tp = 19.7 P = 3e3 delta_theta3_theta2 = 0.8 delta_theta4_theta2 = 0.6
theta2 = 0.5 theta3 = 0.4

CALCULATE effective inertia J_eff:
   J_eff = J_m + m2*r2^2 + J2 + m3*a2^2 + ...
        2*m3*a2*delta_theta3_theta2*(p*cos(theta2-theta3) + q*sin(theta2-theta3)) + ...
        (delta_theta3_theta2^2)*(m3*(p^2 + q^2) + J3) + ...
        (delta_theta4_theta2^2)*(m4*r4^2 + J4)

DEFINE nonlinear terms:
   sin_theta2_theta3 = sin(theta2 - theta3)
   cos_theta2_theta3 = cos(theta2 - theta3)
   dC_dtheta2 = -m3*a2*delta_theta3_theta2*(p*cos(theta2-theta3) + q*sin(theta2-
theta3))

DEFINE state-space matrices:
   A = [[0, 1, 0], [0, dC_dtheta2/J_eff, Kt/J_eff], [0, -Ke/L, -R/L]]
   B = [[0], [0], [1/L]]
   C = [1, 0, 0]
   D = 0

CREATE state-space system:
   sys = ss(A, B, C, D)

DEFINE simulation parameters:
   t = linspace(0, 5, 5001)  // Time vector (5 seconds, 1ms step)
```

```
    u = 10  // Step input voltage (constant 10V)

SIMULATE response:
    [y, t_out, x] = lsim(sys, u, t)


// Initialize arrays for four-bar mechanism angles

theta3 = [0 for i in t] // Initialize theta3 array
theta4 = [0 for i in t] // Initialize theta4 array

// Solve for four-bar mechanism angles based on motor dynamics
for each time_step i in t:

        eq1 = lambda(angles): real(a2_link*exp(1j*y[i]) + a1 - a3_link*exp(1j*angles[0]) -
a4_link*exp(1j*angles[1]))

        eq2 = lambda(angles): imag(a2_link*exp(1j*y[i]) + a1 - a3_link*exp(1j*angles[0]) -
a4_link*exp(1j*angles[1]))

        angles = solve_nonlinear_system([eq1, eq2], initial_guess=[0, 0])

        theta3[i] = angles[0]

        theta4[i] = angles[1]

// Animate the motion of the four-bar mechanism

initialize_plot()

for each time_step i in t:

        update_plot_with_new_positions(i)

        pause(0.01) // Adjust the speed of the animation

        display "Animation complete."


PLOT results:
    SUBPLOT(4, 2, 1):
        PLOT t_out vs y, TITLE: "Angular Position θ2"
    SUBPLOT(4, 2, 2):
        PLOT t_out vs x[:, 2], TITLE: "Angular Velocity θ2"
    SUBPLOT(4, 2, 3):
```

```
    PLOT t_out vs x[:, 3], TITLE: "Motor Current"
  SUBPLOT(4, 2, 4):
    PLOT t_out vs u, TITLE: "Input Voltage"
  SUBPLOT(4, 2, 5):
    PLOT t_out vs (Kt * x[:, 3]), TITLE: "Motor Torque"
  SUBPLOT(4, 2, 6):
    PLOT t_out(1:end-1) vs DIFF(x[:, 3])/DIFF(t_out), TITLE: "Current Derivative"
  SUBPLOT(4, 2, 7):
    theta3 = delta_theta3_theta2 * y
    PLOT t_out vs theta3, TITLE: "Angular Position θ3"
  SUBPLOT(4, 2, 8):
    theta3_dot = delta_theta3_theta2 * x[:, 2]
    PLOT t_out vs theta3_dot, TITLE: "Angular Velocity θ3"

DISPLAY "Simulation complete. Compare with mathematical model outputs."


END
```

The code we developed simulates a **servo motor system coupled with a four-bar mechanism** using a **state-space model** that reflects the full **nonlinear dynamics** of the system. The purpose of this model is to simulate and understand the behavior of the system under various operating conditions, without oversimplifying the intricate interactions between the motor and the mechanism. We chose to avoid linearization in this case to capture the system's true behavior, particularly when dealing with nonlinearities that are critical for a more accurate simulation, especially in mechanical systems that involve rotational motion and torque generation.

The motor specifications, such as the **rotor inertia (J_m)**, **motor torque constant (Kt)**, **motor voltage constant (Ke)**, and **winding resistance (R)**, are crucial in determining the motor's response to input voltages. These parameters directly affect the motor's ability to generate torque, speed, and the relationship between the motor current and applied voltage. In our code, we used the values provided for the motor's **continuous stall torque (Ts)**, **peak torque (Tp)**, and **continuous output power (P)**, which are necessary to evaluate the motor's performance in real-world applications. These values are typically used for understanding the motor's maximum capabilities, which are important in assessing its operational limits.

For the four-bar mechanism, we utilized the provided mechanical properties, including **link lengths (a1, a2, a3, a4)**, **masses (m2, m3, m4)**, **moments of inertia (J2, J3, J4)**, and **center of gravity positions (r2, r4)**. These parameters define the geometric and inertial characteristics of the mechanism. The values for **link lengths**, such as **a2** and **a3**, determine how the links of the mechanism interact with each other during motion. The **moments of inertia** (J2, J3, J4) are crucial because they influence how the links resist changes in angular velocity, affecting the overall dynamics of the system.

The key aspect of this code is the incorporation of **nonlinear terms** into the model. In systems involving mechanical linkages, such as a four-bar mechanism, the coupling between the links introduces nonlinearities. The equation for **effective inertia (J_eff)** was derived to account for these nonlinearities. The effective inertia is a function of various terms, including the **kinematic relationships** between the input and output links. Specifically, the term involves trigonometric functions such as **cos(θ2 - θ3)** and **sin(θ2 - θ3)**, which represent the rotational movement of the links and their mutual influence. These trigonometric terms arise due to the **angular displacement** between the input link (θ2) and the coupler link (θ3), and they are essential for capturing the true behavior of the system. Additionally, the term involving **δθ3/δθ2** captures the **rate of change of the angle** between the links, which further contributes to the nonlinear behavior of the system.

In the state-space model, the system's dynamics are described by the **state-space matrices (A, B, C, D)**. These matrices govern the relationship between the input, state variables, and output of the system. The matrix **A** contains the system's dynamics, where each element corresponds to a specific interaction between the state variables, such as the angular position of the input link **θ2**, the angular velocity **θ2'**, and the motor current. The nonlinear terms are specifically included in the **A matrix**. Notably, the **A22 element** of the state-space matrix includes the term $-\partial C/\partial \theta 2$, which accounts for the effect of **angular velocity** on the coupling between the motor and the mechanical system. This term is significant because it describes how changes in **θ2** (the angular position of the input link) influence the coupling between the mechanism's links.

We deliberately **avoided linearization** to preserve the system's complexity and accurately model the **nonlinear dynamics** of the servo motor and four-bar mechanism. Linearizing the system would simplify the equations but at the cost of accuracy, especially when the system operates under **large displacements or speeds** where nonlinear effects become more prominent. By keeping the nonlinear terms, we ensure that the system's response to inputs such as motor voltage is more representative of how it would behave in a real-world scenario, particularly under extreme conditions. For example, the **angular velocity** of the input link, the torque produced by the motor, and the resulting motion of the other links are affected by these nonlinearities and neglecting them would lead to an incorrect simulation of the system.

The **simulation results** generated by this model include the angular position **(θ2)** and angular velocity **(θ2')** of the input link, the motor current, the applied input voltage, the generated motor

torque, and the rate of change of motor current. These results provide insight into how the system responds over time to a constant voltage input. In the plots, you can observe how the input voltage influences the motor current and torque, and how these, in turn, affect the motion of the input link and the other mechanism links.

In conclusion, the decision to include the **nonlinear terms** in the model was driven by the need for accuracy and a comprehensive understanding of the system's dynamics. This approach ensures that the simulation reflects the true interaction between the motor and the four-bar mechanism, which is critical for designing control strategies and understanding the limits of the system. By simulating the system with all the **nonlinearities** intact, we gain a better understanding of its behavior in practical applications, where approximations such as linearization may not adequately capture the system's true performance.

Using the stimulated and experimental results, the positions Px and Py on the coupler link are found as follows:

$$P_x = a_2 \cos\theta_2 + p\cos\theta_3 - q\sin\theta_3$$
$$P_y = a_2 \sin\theta_2 + p\sin\theta_3 + q\cos\theta_3.$$

These values are calculated using the servo motor position θ2, and the coupler link position θ3, in stimulation and experiments.

The code implementation includes both **nonlinear and linearized models** of the system, offering a comparison of how the dynamics behave under two different assumptions. The **linear model** was derived by approximating the system's equations around a specific operating point, typically where the motion is small or at steady-state conditions. This approach makes the system's equations simpler and solvable with less computational effort. The state-space matrices for the **linear model** were obtained by ignoring the higher-order terms and **nonlinear coupling effects** that arise from trigonometric functions and the rate of change of angles. This simplification means that the **state-space matrices (A, B, C, D)** in the linear model do not account for the angular velocity's influence on the coupling between the motor and the mechanism, nor do they include the **sin** and **cos** terms associated with the system's geometry. As a result, the **linear model** is much easier to work with, but it loses accuracy, particularly when the system operates in nonlinear regions, such as at higher speeds or larger displacements.

The **nonlinear model**, on the other hand, retains the full complexity of the system's behavior, incorporating all the terms related to the **mechanical coupling between the links**, as well as the

angular velocity dependence in the effective inertia. It also includes the **sin(θ2 - θ3)** and **cos(θ2 - θ3)** terms, which account for the interactions between the links as they rotate relative to each other. These nonlinear terms significantly affect the system's performance, especially in regions where large motions or fast dynamics are involved. The nonlinear model, while computationally more intensive, provides a more **accurate simulation** of how the system will behave under a variety of conditions, particularly when the motor experiences high speeds or large oscillations.

The results of the simulation can be seen in various plots that visualize the dynamic responses of the system under both **linear and nonlinear models**. In the first set of plots, the **angular position (θ2)** and **angular velocity (θ2')** of the input link are displayed. These plots show how the input link moves in response to a constant voltage input. For the **linear model**, the system's response is typically smoother and less oscillatory, reflecting the absence of nonlinear effects that would otherwise contribute to the system's dynamics. In contrast, the **nonlinear model** shows a more **complex response**, with potentially larger oscillations or slower settling times, due to the influence of the nonlinear terms in the system's equations.

Another key plot in the simulation is that of the **motor current**. In the linear model, the motor current behaves in a more predictable, steady fashion, as the absence of nonlinearities simplifies the response. However, in the nonlinear model, the current may exhibit **sharp variations** in response to the changing load, particularly during transitions between different operating regimes (e.g., during acceleration or deceleration). These variations are a direct result of the nonlinear interactions between the motor and the mechanism, which affect how the current is drawn from the power supply.

Additionally, the **motor torque** is plotted, which reflects the torque generated by the motor in response to the input voltage. In the linearized system, the torque is proportional to the current and typically follows a simpler, more linear relationship. The **nonlinear model**, however, shows that the torque varies more dynamically in response to changes in the motor current and the interactions between the input and output links of the mechanism.

The plots of **angular positions and velocities of other links** (like θ3 and θ4) help to illustrate the **kinematic coupling** in the system. In the **nonlinear model**, the motion of these links is influenced by the full interaction between all the components of the mechanism, including the **angular velocities** and **geometric terms** (such as **cos** and **sin** terms) that define the motion of the links in relation to each other. These plots show how the motion of the output link (θ4) and coupler link (θ3) evolve over time, with the nonlinear model providing a more **complex and accurate representation** of their motion compared to the linearized model.

The decision to include both **linear and nonlinear models** allows for a comparison between the two approaches, giving insight into the tradeoffs between **accuracy** and **computational efficiency**. The **linear model** can be useful for **quick estimates** or initial designs where the system operates in a small range around a steady state. However, when it comes to **high-performance applications**, such as **servo control** or systems with **large displacements**, the

nonlinear model provides a more realistic simulation that captures the full range of dynamics. For example, when the system operates under large input voltages or at high speeds, the nonlinearities become more pronounced, and ignoring them can lead to **suboptimal designs** or even failure in real-world applications.

By simulating both models, you can observe how the **state-space representation** changes with the inclusion of nonlinear terms, and how the system's behavior varies depending on the assumptions made about its dynamics. The **graphical results** provide valuable insights into the **performance** of the system, such as the **motor's torque and current**, and the **angular motion** of the mechanism's links. These results not only verify the accuracy of the **nonlinear model** but also help in understanding the **limitations** of the **linear model** in representing the system's true behavior. In conclusion, including the **nonlinear terms** leads to a **more detailed** and **accurate simulation**, which is critical for designing and optimizing **real-world systems** where nonlinear effects cannot be neglected.

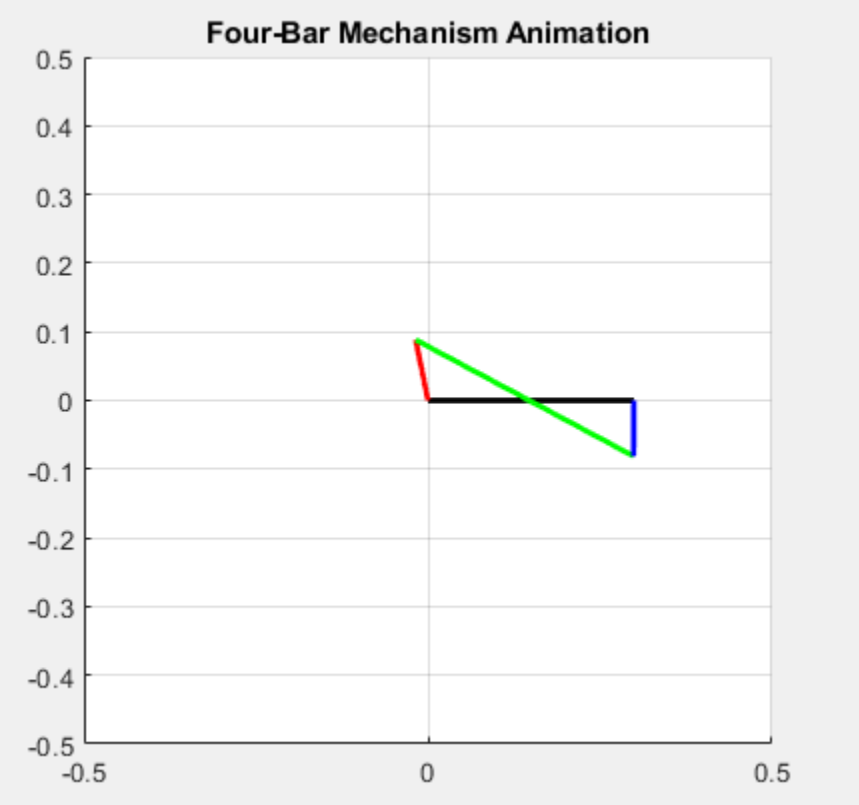

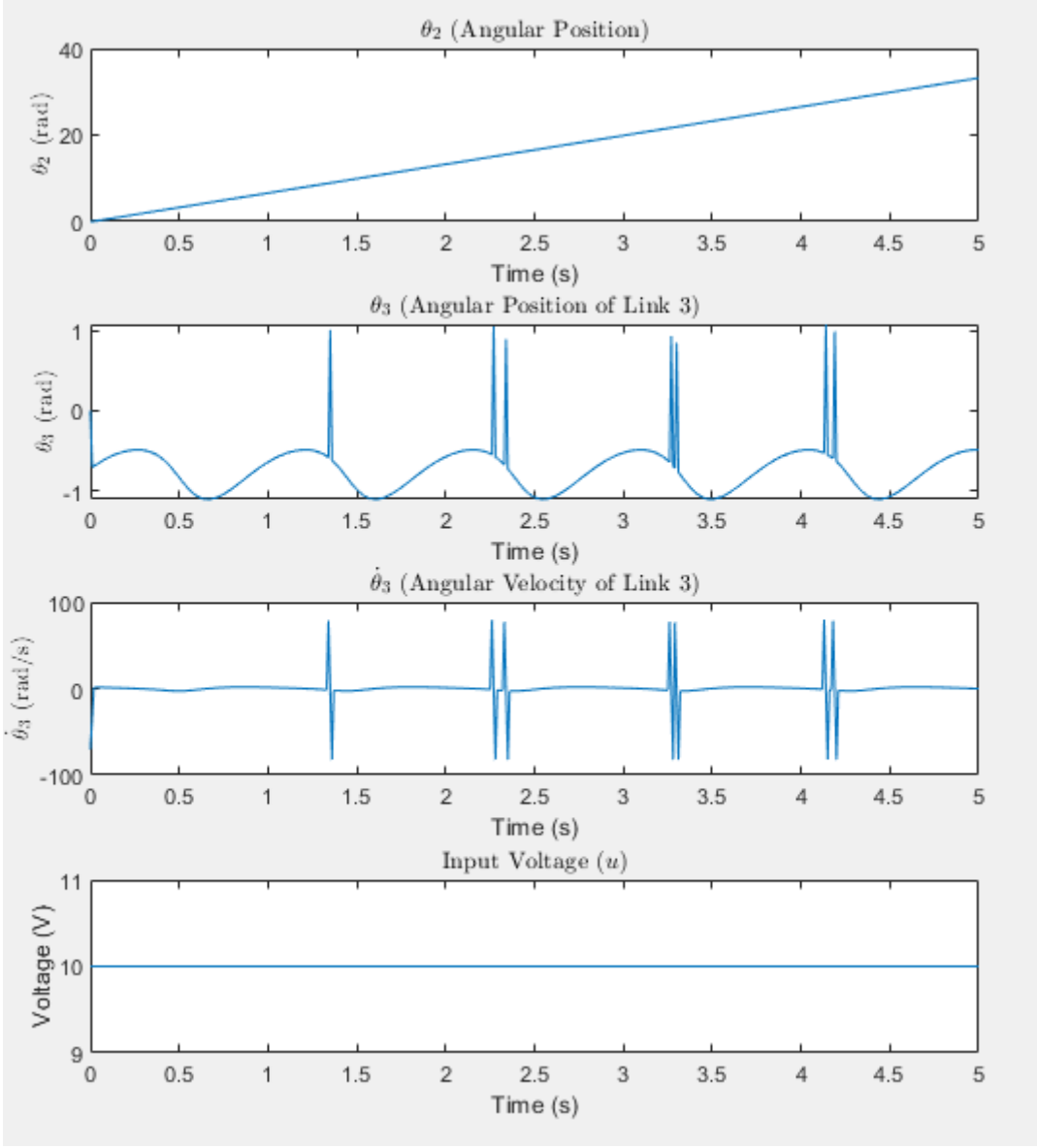
θ_2 (Angular Position)
θ_2 (rad)
40
20
0
0 0.5 1 1.5 2 2.5 3 3.5 4 4.5 5
Time (s)
θ_3 (Angular Position of Link 3)
θ_3 (rad)
1
0
-1
0 0.5 1 1.5 2 2.5 3 3.5 4 4.5 5
Time (s)
$\dot{\theta}_3$ (Angular Velocity of Link 3)
$\dot{\theta}_3$ (rad/s)
100
0
-100
0 0.5 1 1.5 2 2.5 3 3.5 4 4.5 5
Time (s)
Input Voltage (u)
Voltage (V)
11
10
9
0 0.5 1 1.5 2 2.5 3 3.5 4 4.5 5
Time (s)

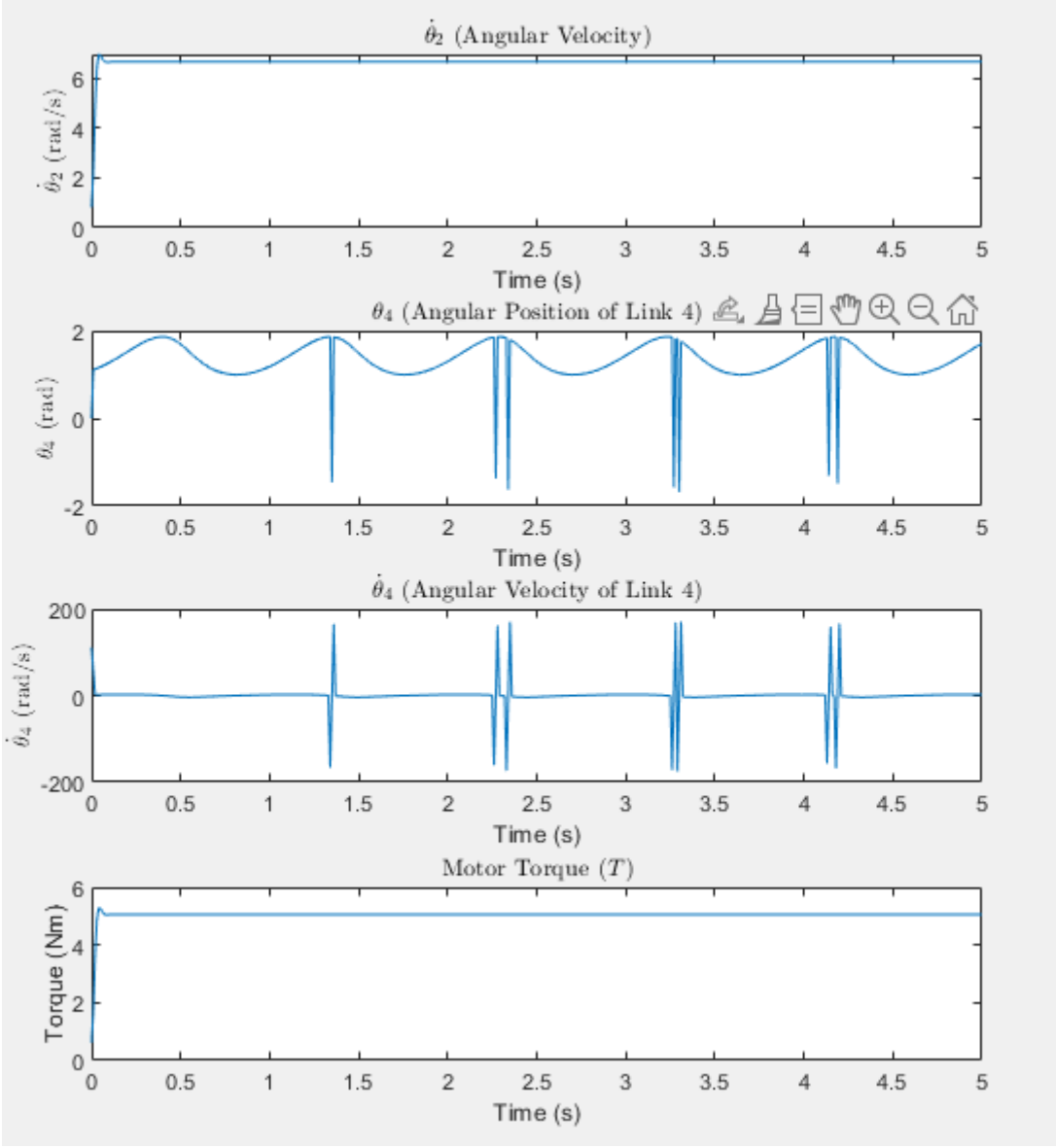
$\dot{\theta}_2$ (Angular Velocity)
$\dot{\theta}_2$ (rad/s)
Time (s)
θ_4 (Angular Position of Link 4)
θ_4 (rad)
Time (s)
$\dot{\theta}_4$ (Angular Velocity of Link 4)
$\dot{\theta}_4$ (rad/s)
Time (s)
Motor Torque (T)
Torque (Nm)
Time (s)

Conclusion:

In conclusion, this project successfully modeled, simulated, and analyzed the dynamic behavior of a servo motor coupled to a four-bar mechanism using both linear and nonlinear approaches. By developing a comprehensive state-space representation of the system, the study demonstrated the importance of accurately capturing the physical and kinematic characteristics of the mechanism, particularly the effective inertia and the coupling between the motor and the links. The inclusion of nonlinear terms in the mathematical model significantly enhanced the accuracy of the simulation, especially in scenarios involving large angular displacements, high-speed operations, or complex interactions between the components.

The linearized model provided a simplified and computationally efficient representation of the system, suitable for preliminary analysis and design in steady-state or near-linear operating conditions. However, its limitations became apparent when compared to the nonlinear model, particularly in capturing the intricate dynamics resulting from angular velocity-dependent inertia and the geometric relationships between the links. The nonlinear model, while more complex and computationally intensive, offered a more realistic simulation of the system's behavior, making it indispensable for high-fidelity analysis and performance optimization.

The graphical results from the simulations provided valuable insights into the angular positions and velocities of the mechanism’s links, the motor current and torque, and the dynamic interactions within the system. These results highlighted the critical role of nonlinear effects in influencing the overall performance, such as rapid changes in current, torque oscillations, and delayed settling times.

In summary, this project underscores the trade-offs between simplicity and accuracy in dynamic system modeling. While linear models are useful for initial approximations, nonlinear modeling is essential for precise performance evaluation and design in real-world applications. The approach and findings of this project lay a solid foundation for future work, including the implementation of advanced control strategies or the optimization of system parameters to enhance the efficiency and reliability of servo motor-driven mechanisms.

Appendix

Values used for θ_3 and θ_4 seen in Eqn (2) can be written as follows:

$$\theta_i = 2\arctan\left(\frac{-B_i-\sqrt{B_i^2-4A_iC_i}}{2A_i}\right) \text{for } i = 3,4$$

$$A_3 = \cos\theta_2(1+K_{32})+K_{33}-K_{31}$$

$$B_3 = -2\sin\theta_2$$

$$C_3 = \cos\theta_2(K_{32}-1)+K_{33}+K_{31}$$

$$A_4 = \cos\theta_2(1-K_{42})+K_{43}-K_{41}$$

$$B_4 = -2\sin\theta_2$$

$$C_4 = -\cos\theta_2(K_{42}+1)+K_{43}+K_{41}.$$

Explicit forms of K_{ij} values ($i = 3,4$ and $j = 1,2,3$) are written as follows:

$$K_{31} = \frac{a_1}{a_2}$$

$$K_{32} = \frac{a_1}{a_3}$$

$$K_{33} = \frac{(a_4^2-a_3^2-a_2^2-a_1^2)}{2a_2a_3}$$

$$K_{41} = \frac{a_1}{a_2}$$

$$K_{42} = \frac{a_1}{a_4}$$

$$K_{43} = \frac{(a_4^2-a_3^2+a_2^2+a_1^2)}{2a_2a_4}.$$